J. Fluid Mech. (1968), *vol.* 31, *part* 4, *pp.* 801–814
Printed in Great Britain

Experimental studies in magneto-fluid dynamics: pressure distribution measurements around a sphere

By T. MAXWORTHY†
Jet Propulsion Laboratory
California Institute of Technology, Pasadena, California

(Received 27 July 1967)

Measurements of the pressure distribution around a sphere placed in aligned magnetic and velocity fields show that an increase in drag is mainly due to a decrease in the pressure on the base of the body. When magnetic forces are large compared to inertia forces, this decrease is due to a loss in total pressure along streamlines just outside the surface boundary layer and an acceleration of the flow to a velocity much larger than the reference velocity. Separation of a viscous boundary layer takes place behind the equator and still, to a large extent, controls the magnitude of the base pressure and the drag experienced by the sphere. A model consistent with these findings is presented.

1. Introduction

A knowledge of the forces on bodies in magneto-fluid dynamic flows (Yonas 1966, 1968) is a crucial first step in understanding the fluid motions around them. Ideally, one would next like to probe the near flow field in order to determine in detail the cause of these forces and attempt to expose some underlying principles which could be of use in constructing theoretical models. Unfortunately, the introduction of large probes near to the body would probably tend to destroy the features under observation. As a substitute for this step a quantity should be measured which both tells something about the flow and can also be used to understand the effect of external probes. The determination of the pressures on the surface of a body is such a measurement. By drawing on experience gained from similar measurements in ordinary flow, e.g. Fage (1937) and by applying some of the simple physical ideas of magneto-fluid dynamics, it is possible to construct a reasonably accurate first picture of the gross features of the velocity and magnetic fields. This must then be modified by further measurements within the flow itself. If during these latter probings it is found that the pressure distribution on the body is drastically changed, then such techniques must be discarded or at least modified to remove the interferences.

Just the results of the measurement of the distribution of surface static and total pressure around a sphere in an aligned fields' magneto-fluid dynamic flow are presented in this paper; the problem of external measurements is left for presentation in a future paper.

† Present address: Departments of Aerospace and Mechanical Engineering, University of Southern California, Los Angeles, California.

Only a moderate amount of information is available in the literature on the problem under consideration. Most effort has been expended on cases which are not readily amenable to experimental study. Accurate experiments can only be performed in fluids which are of small kinematic viscosity and relatively small electrical conductivity (e.g. sodium, mercury, sodium-potassium eutectic, etc.). For the body size (1·27 cm dia.), and velocities and magnetic fields obtainable in the J.P.L. liquid sodium tunnel, the characteristic parameters have the following ranges of values: the Reynolds number ($R = Ud/\nu$) $2{\cdot}6 \times 10^4$ to $9{\cdot}1 \times 10^4$; the interaction parameter ($N = \sigma B^2 d/\rho U$) 0 to 40; the magnetic Prandtl number ($P = \mu\sigma\nu$), fixed for any particular fluid, is $7{\cdot}16 \times 10^{-6}$† for liquid sodium at 275 °F. Other convenient parameters can be constructed from these basic ones: the Hartmann number[2] ($H^2 = (RN)$), the magnetic Reynolds number ($R_m = RP$), the Alfvén number ($\alpha = (N/R_m)^{\frac{1}{2}}$; their conventional interpretation is well known.‡ It would appear that, in general, viscous effects are unimportant and that magnetic forces dominate all the others. From experience in ordinary flow, it is known that such a simple statement must be considered very carefully: for example, at very large R the formation of boundary layers and their subsequent separation have changed all preconceptions about almost inviscid fluid flow. Powerful unifying concepts, like the boundary layer, have not been well established in magneto-fluid dynamic flows so the existence of regions within which similar simplifications can be made should be anticipated. In the model to be described such an approach is taken, but since all of its detailed features are not yet clear, it must be considered as a 'first-order' model.

Most previous authors have considered cases which do not satisfy the experimental conditions because they treat the limit of a viscous fluid. However, two previous approaches are of use and contain, in small measure, some of the features of the experimental flow. Based on the required non-linear behaviour of the Bernoulli function ($P^0 = P + \frac{1}{2}U^2$),§ both Tamada (1962) and Childress (1963) derived a consistent inviscid model. The prime consideration is the existence of a forward stagnant region within which the pressure is constant at a value equal to the upstream total pressure. Because their inviscid model does not allow negative values‖ of P^0, in violation of uniform downstream boundary conditions, their rearward flow is of limited usefulness. Further work by Tamada (1961) used an Oseen linearization mainly to describe flow in the neighbourhood of the body. Despite this seemingly poor assumption, it does, in fact, qualitatively predict one feature of the experimental flow; the acceleration of fluid around the equator

† Here U, ρ, ν, σ and μ are the fluid velocity, density, kinematic viscosity, electrical conductivity and magnetic permeability; d is the sphere diameter and B the applied magnetic flux density.

‡ The conventional interpretation of R_m as a measure of the distortion of the magnetic field should be modified by realizing that this is only true for a given velocity field. If the velocity is also a function of magnetic field (e.g. N), then the magnetic field change will also depend on N.

§ P^0 is the total pressure, P the static pressure and U the velocity.

‖ All pressures use the approach stream static pressure (P_∞) as a reference except where noted. Negative values thus refer to a pressure less than this reference. The subscript ∞ refers to conditions far upstream.

and the production of a forward stagnant region. For high sub-Alfvénic flows, it also gives some clue to the flow to be expected far upstream, where the Oseen approximation should be valid. Apart from an expected retardation of the flow on the axis, there is a velocity greater than the free-stream value at a radius of the order of the body size. As this layer of high velocity approaches the body, it thins; the velocities become larger as it sweeps over the maximum diameter of the body. Identical features appear in the work of Lary (1962) who considered linearized flow over slender bodies. Again this work showed the existence of a stagnant flow upstream and an accelerated flow at larger radii, producing a large negative pressure over the rear of the body. Horlock (1963), using an experimental analogy, found a similar result.

2. Apparatus and experiments

The device shown in figure 1*a* was mounted in the centre of the test section of the J.P.L. Liquid Sodium Tunnel (Maxworthy 1961, 1967). It is a sphere cut into two pieces, one of which is stationary and is mounted on a support member, while the other can be rotated with respect to the stationary section. A small hole is drilled in the rotating piece and is connected through various oil-filled channels to one side of the diaphragm of a calibrated 'Pace', variable reluctance, pressure

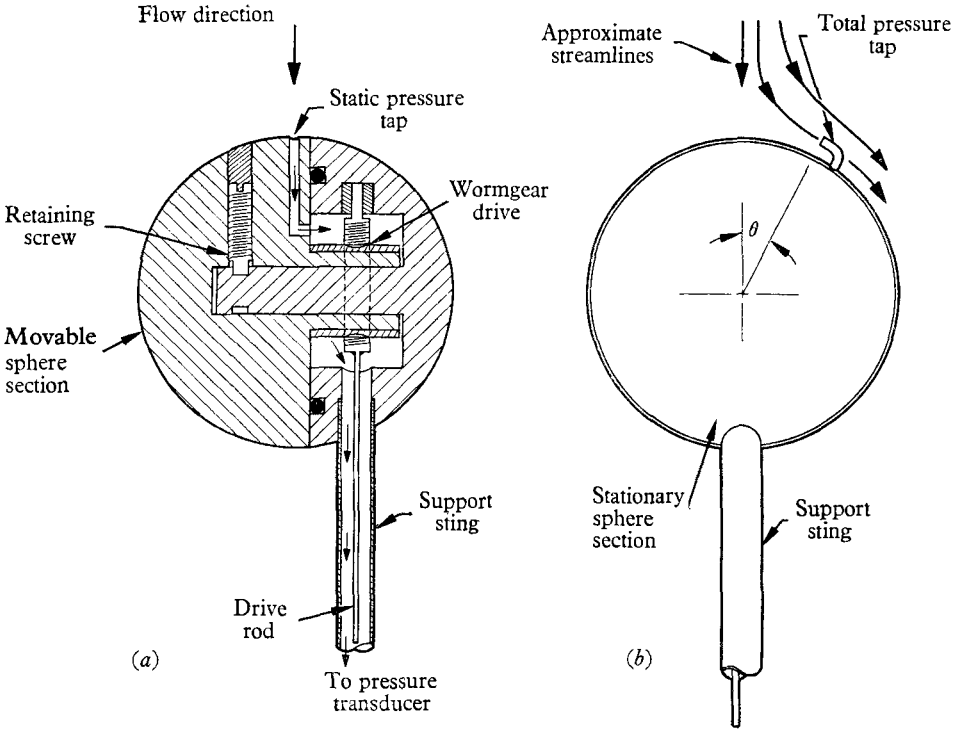

FIGURE 1(*a*). Side section of the split sphere showing the mechanism for rotating the moving section and transmitting the pressure from the liquid sodium to the pressure transducer. (*b*) Front view showing the location of the tube used to measure the angular distribution of local total pressure.

transducer. The other side of the diaphragm is connected to a reference pressure, in this case the initial total pressure of the flow as found at the entrance of the nozzle leading to the test section. Again the pressure is transmitted from the heated sodium to the room temperature transducer through tubes filled with an inert silicone oil. The electrical measure of this pressure difference is fed to the y axis of an x–y plotter. A potentiometer is attached to the drive motor of the rotating sphere and this output is fed to the x axis of the plotter. Thus $P_\theta - P_\infty^0$† is obtained directly as a function of the angular position (θ) of the pressure hole around the sphere. Figure 1*b* shows this same sphere slightly modified to measure the total pressure (P_θ^0) a small distance from the sphere surface. A piece of thin-walled hypodermic tubing is pressed into the pressure tap and bent so that it is tangential to the sphere surface; i.e. the plane of its opening is normal to the local stream velocity.

All the further details necessary to describe the experimental technique, e.g. pressure measuring system, velocity, flow rate, magnetic field determination, etc., are to be found in Maxworthy (1967), and only the basic ideas need be repeated here. The approach velocity is measured using a conventional Pitot-static probe, connected by oil-filled lines to the above-mentioned 'Pace' pressure transducer. This velocity is calibrated against the output of a 'cross-field' electromagnetic flow meter, which is then used as the primary means of setting a known flow in the test section. The applied magnetic field is measured using a calibrated 'Hall type' of device located adjacent to the test section and within the solenoid creating the aligned magnetic field.

3. Results

Initially, considerable difficulty was experienced in reproducing the classical features of laminary flow about a sphere with no magnetic field. This was traced, in a separate wind tunnel investigation, to a complicated, and previously untreated, three-dimensional boundary-layer transition and separation phenomenon created because the boundary layer had to flow over the slightly raised step at the split between the two halves of the sphere. Using knowledge gained from this subsidiary experiment, the sphere geometry was changed to that shown in figure 1*a*. After the change, the difficulty existed only at the highest flow rates, so they were not used in the present study (except where noted). Only the results at flow rates which give the known behaviour with no magnetic field are considered.

The basic features of the results are given in figure 2*a*. They describe in a general way the changes which take place in the static pressure profiles as the interaction parameter, N, is increased. Some detailed profiles are shown in figures 3 and 4. Several changes take place at the same time and can best be described by realizing that the total drag force on the body is made up of three parts. Referring to figure 2*b* the portions $0 < \theta < \theta_s$ and $90° < \theta < 180°$ contribute positively to the drag; the portion $\theta_s < \theta < 90°$ negatively. As N is increased, the base pressure increases resulting in a decreased contribution of the base (C_{D_B})‡ to the total

† The subscript θ refers to conditions at the angular position θ on the sphere surface, measured from zero at the front stagnation point.

‡ All C_D quantities are defined on the legend to figure 2*a*.

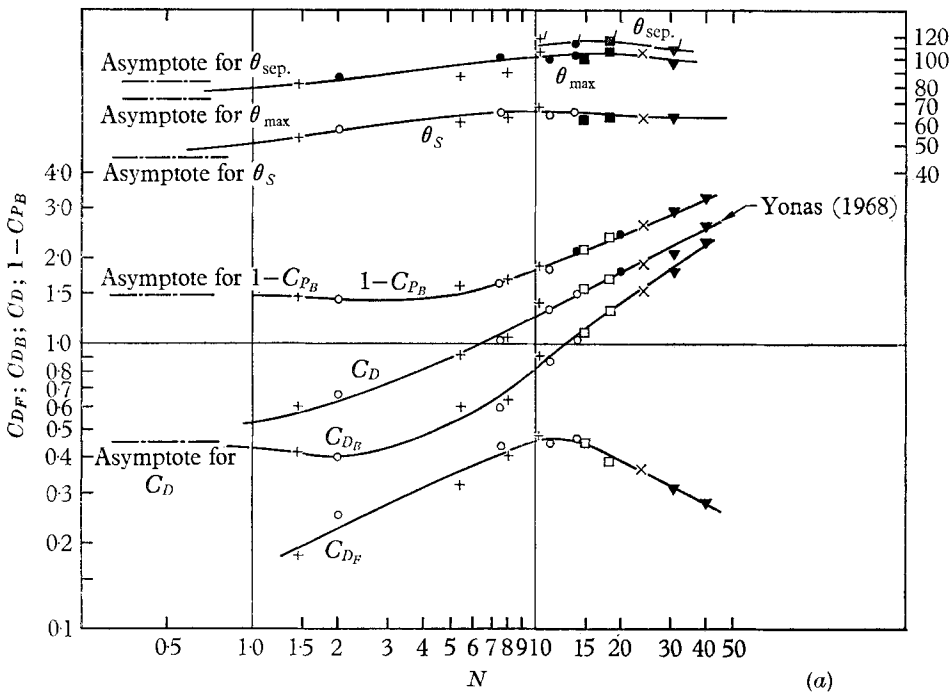

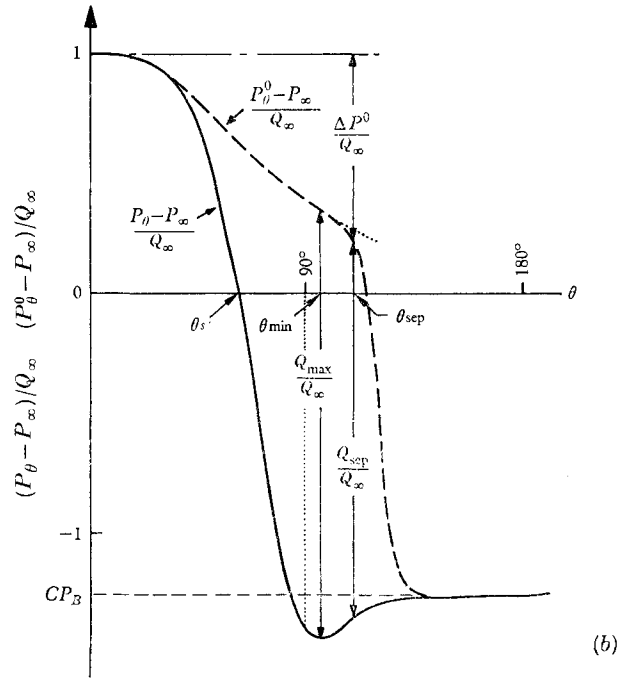

FIGURE 2. (*a*) A composite figure to show all of the major changes which take place as the interaction parameter, N, is increased. Here, C_D is the overall drag coefficient $D/\frac{1}{2}\rho U_\infty^2 \frac{1}{4}\pi d^2$; C_{D_F} is the drag coefficient of the front half of the sphere only, referred to the upstream static pressure; C_{D_B} the drag coefficient of the rear half of the sphere only; C_{P_B} is the base pressure coefficient $P_B - P_\infty / \frac{1}{2}\rho U_\infty^2$. (*b*) Defines the angle at which the local static pressure is the same as that upstream (θ_s), the angle at minimum pressure (θ_{max}), and the angle at boundary-layer separation (θ_{sep}).

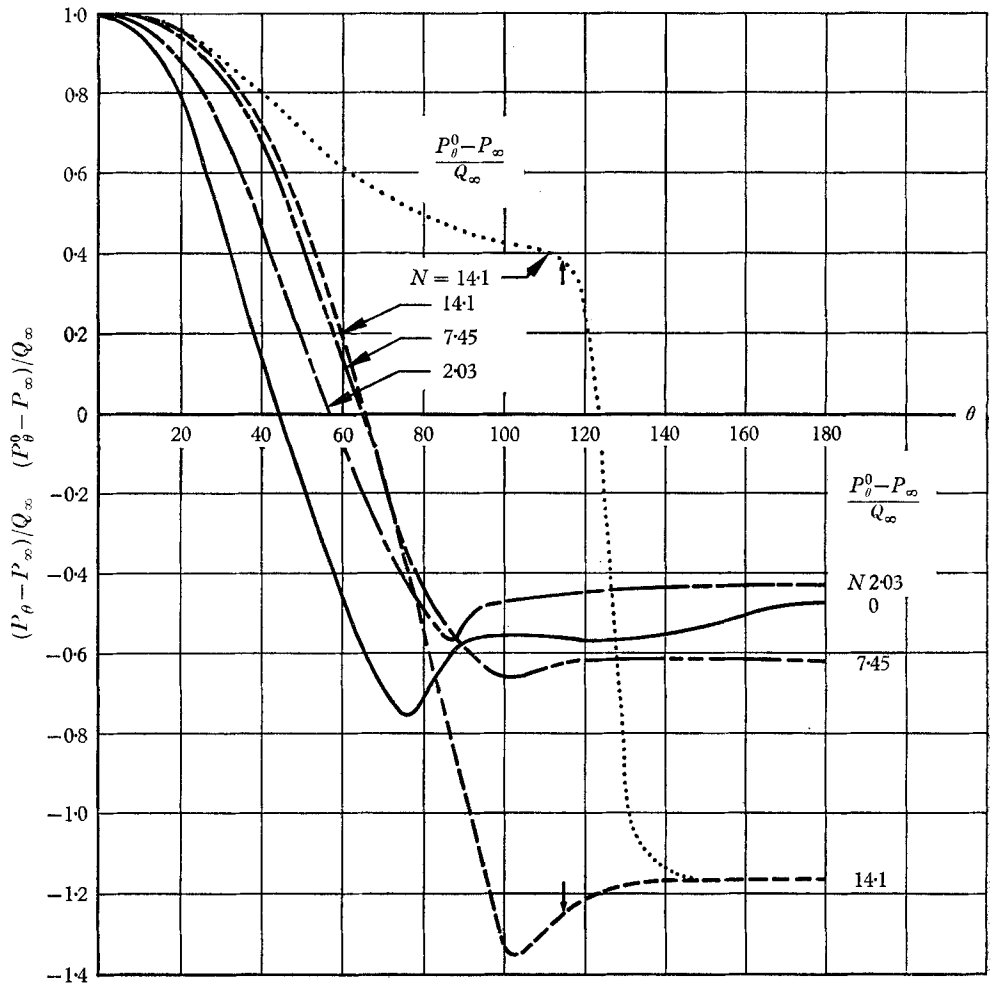

FIGURE 3. (*For legend see facing page.*)

drag (C_D). However, C_D does in fact increase because of an increased contribution from the front of the sphere (C_{D_F}). C_{D_F} increases because the pressure distribution is becoming more uniform at a value of P^0_∞ and because it covers a greater portion of the front surface, i.e. θ_s is increasing. As N increases further, the base pressure now begins to decrease so that both contributions C_{D_B} and C_{D_F} are increasing. From now on C_D and C_{D_B} continue to increase indefinitely as the base pressure continuously falls. C_{D_F}, however, reaches a maximum and then begins to decrease and presumably becomes negative as N continues beyond the range of the experiment. This result is explained by the continued existence of the region of suction between θ_s and 90°. Since the pressure between $\theta = 0$ and θ_s cannot exceed P^0_∞,† and since θ_s remains constant at 63°, the positive contribu-

† Along the axis of symmetry the current density, j_θ, is zero; the total pressure can only change due to viscous effects. For these high R flows such effects are small. Therefore the nose stagnation pressure is essentially the same as the upstream stagnation pressure.

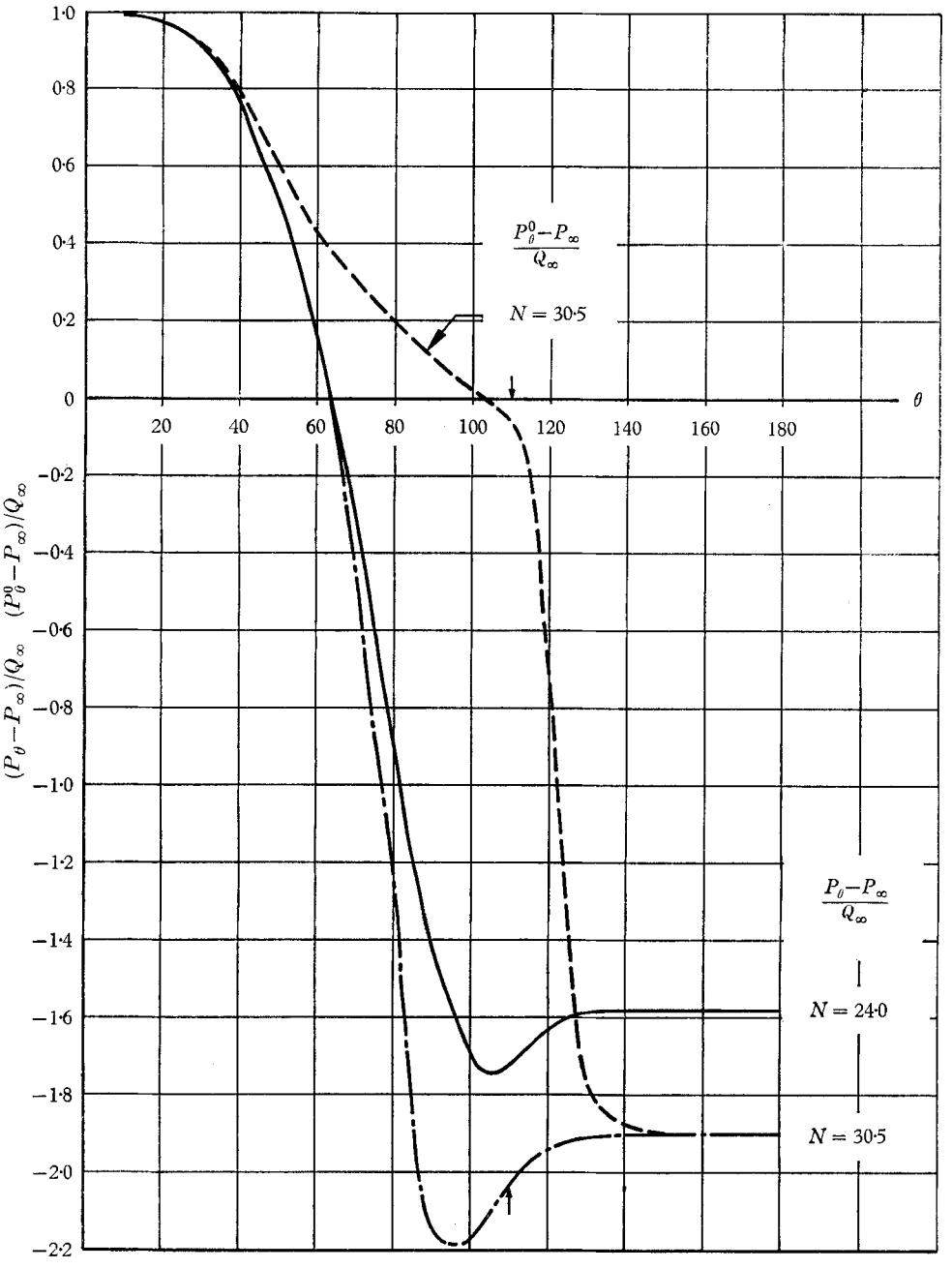

FIGURES 3 and 4. $(P_\theta - P_\infty)/Q_\infty$ *vs.* θ for various N. $(P_\theta^0 - P_\infty)/Q$ *vs.* θ to show general character of these curves. $R = 6{\cdot}4 \times 10^4$.

tion from the nose reaches a steady value. The negative contribution continuously erodes this positive quantity as P [at θ equals 90 degrees] rapidly decreases. Eventually positive pressure on the nose must be completely nullified by the suction and, *unless some new drastic change takes place in the present trend*, C_{D_F}

will become more and more negative. Reasonable extrapolation of the present results shows that C_{D_F} is approximately zero when N is about 100.

All of these gross statements can be verified in detail from the actual profiles of figures 3 and 4. Also plotted in figure 2*a* is the behaviour of the location of point of lowest pressure ($\theta_{\max}$). For small N it rises from 73° to 105° and then falls to 100°. The position of separation $(\theta)_{\text{sep}}$† follows the same trend but with numerical values about 10° larger.

The base pressure, at values of θ larger than that at separation, is constant. As in flow with no magnetic field the base pressure is produced by a complex interaction between the pressure field of an inviscid outer flow, created by motion over the body and a separated wake, and the separation of the boundary-layer flow which itself depends on the outer flow pressure field. A final flow pattern is produced which is compatible with both requirements. Of course, in calculating the outer flow and boundary-layer flow to separation for the present case, magnetic forces now play an important role. Since the similar situation with no magnetic field is still considered an unsolved and controversial problem, it seems unlikely that the case with magnetic field will be solved until a complete understanding of the former is obtained. However, it is possible to conclude that at large N separation occurs behind the sphere equator and still, in some sense, controls the magnitude of the base pressure.

These results are further borne out by measurements of the local stagnation pressure. The small inserted probe was designed to be always outside the conventional boundary layer, i.e. in the outer potential flow, except after the point of separation. Of course, there is no guarantee that this will be true with magnetic field applied because boundary-layer behaviour is unknown under such circumstances. These profiles are also shown superimposed on figures 3 and 4. With no magnetic field P_θ^0 is constant until separation occurs, after which it drops precipitously to the base pressure. Separation is assumed to have started when the flow has lost 1 % of its initial total pressure. With magnetic field applied, P_θ^0 slowly decreases with θ until in the neighbourhood of the equator it is almost constant; just beyond this point, separation occurs and P_θ^0 again drops rapidly. Again separation is assumed to occur after 1 % of P_∞^0 has been lost from the almost constant value of P^0 just before separation. Apart from knowing point by point values, two useful observations can be made. We can determine the total pressure loss suffered by streamlines that just pass outside the equator,‡ and find this trend with N. Such results are plotted in figure 5 and are denoted as $\Delta P^0/Q_\infty$. Figure 2*b* shows how this is precisely defined as the total pressure loss up to the separation point. As N increases, this quantity also increases and accounts for some of the static pressure change to separation. Assuming that the static pressure at the surface and at the small probe are the same, then the difference between

† Separation is difficult to determine from static pressure profiles alone. The values plotted are in fact obtained from the measurements of local total pressure described in later paragraphs.

‡ It should be realized that because the probe is situated a reasonable distance from the sphere surface, it measures the total pressure loss suffered along different streamlines at each value of θ.

the measured local total and static pressure is the *local* dynamic head from which one can calculate the local velocity a small distance from the surface. For small θ (up to about 30°) the velocity is very small, much smaller than that of the

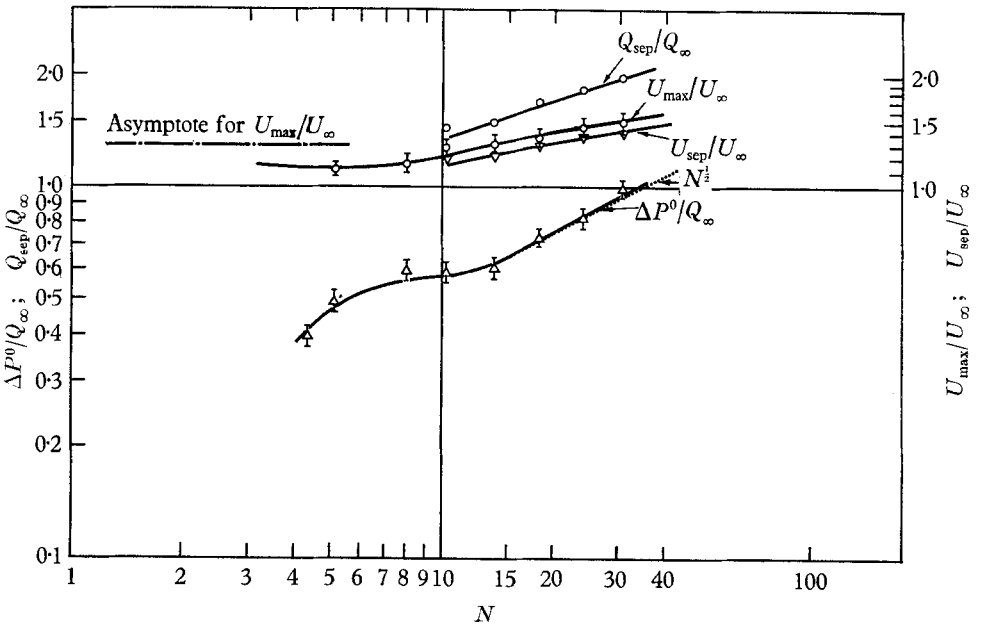

FIGURE 5. Loss in total pressure to separation ($\Delta P^0/Q_\infty$); maximum velocity (U_{max}/U_∞); velocity (U_{sep}/U_∞) and dynamic pressure (Q_{sep}/Q_∞) at separation. Figure 2*b* defines these quantities in terms of the profiles shown in figures 3 and 4.

corresponding potential flow, indicating the existence of a stagnant region ahead of the sphere in this neighbourhood. As θ increases, the velocity increases until it reaches a maximum ($Q_{max} = \frac{1}{2}U^2_{max}$) at θ_{max}. In figure 5 this maximum velocity is plotted as a function of N. At small N it is less than the value for $N = 0$ but increases slowly as N increases beyond 6 until it reaches a value of 1·5 at $N = 30{\cdot}5$. The trend of the results indicates that this velocity will continue to increase as N is further raised in value. Also plotted is the velocity at separation itself and the dynamic pressure represented by this velocity. Extrapolation of these trends to larger N (of the order of 100) show that when $\Delta P^0/Q_\infty$ and Q_{sep}/Q_∞ are added, a value in precise agreement with the extrapolation of the base pressure curve C_{P_B}† is obtained, indicating that such an extrapolation is consistent if the measured trends do not change drastically before N of 100 is reached. Thus the variation in static pressure is seen to be due to two causes: a change in velocity outside the boundary layer, as is usually found in ordinary flow, and a decrease in total pressure on streamlines which flow around the body. The causes of these changes are to be found in the discussion section.

Further documentation of the importance of boundary-layer structure and its

† Assuming that the small pressure difference between the base pressure and the pressure at separation is constant.

mode of separation can be gained from results at high flow rates which have not been used yet. They were not presented with the previous data because they gave results with no magnetic field which did not agree with either classical, axisymmetric laminar, transitional or fully turbulent data.† In the present case as the thin boundary layer flows over the slight step between the two halves of the sphere, it undergoes a transition to turbulence on that side of the sphere, and the separation wants to move beyond the equator. On the other side of the sphere the layer is still laminar and wants to separate before the equator. The competing pressure fields can communicate readily with one another and produce in the plane of the pressure tap a pressure distribution which has a base pressure a little higher than the laminar value and a minimum pressure dip which looks more like the fully turbulent case. When this complex boundary-layer structure is also subject to a magnetic field, it performs unlike the previous laminar cases. At a given value of N the base pressure is lower than the laminar case and the drag coefficient higher. It introduces a Reynolds number effect which is undoubtedly premature but which must eventually take place when completely laminar boundary layers undergo a natural transition to turbulence at higher values of R than those obtained in these experiments. These results have not been plotted on an already complicated figure 2*a*, but they should be borne in mind when extension to still higher R is contemplated, or if axisymmetric, turbulence-producing trips are to be introduced to show the effect of turbulent boundary layers at lower R.

4. Discussion

This section is used to discuss the significance of the presented results and at the same time attempt to construct a 'first-order' model of the flow field at large N using four sources of information: (A) the present results, (B) the drag results of Yonas (1968), (C) the results of magnetic field measurements previously described by Maxworthy (1961), Ahlstrom (1963), and the theoretical description of Tamada (1961), (D) the similarity to flow created as a body moves through a rotating or a stratified fluid.

The significant information can be conveniently summarized in order to make the steps of the deductive process clearer.

(A) (i) A region of stagnant fluid exists from 0° to approximately 30°. Beyond this the flow slowly and then more rapidly accelerates to a large velocity just before separation. The velocity just before separation is a weakly increasing function of N. (ii) Separation of the boundary layer takes place beyond the equator, suggesting a lateral force making fluid particles move radially inwards against the applied magnetic field but not necessarily against the distorted magnetic field created by the motion. (iii) A large loss in P^0, which depends on N, has been suffered along streamlines which pass just outside the equator. The radial distribution of P^0 is not known in the equatorial plane except that it must approach P^0_∞ for large radii. Similarly there is a large radial static pressure difference in the plane of the equator which cannot be balanced by centripetal acceleration,

† As described by Fage (1937) and by a separate, as yet unpublished, study by the present author.

as in ordinary potential-like flow. We must postulate a radial Lorentz force to balance a radial pressure gradient, the magnitude of which must become very large as N increases. (iv) The increase in drag coefficient of the sphere is mainly due to a rapid decrease in the base pressure. The contribution from the front half of the sphere is eventually negligible.

(B) For large N the drag coefficient is proportional to $N^{\frac{1}{2}}$ independent of body shape and satisfies a simply solid body tunnel blockage correction. This suggests the existence of long relatively stagnant regions ahead of and behind the body.

(C) Magnetic field measurements averaged over a plane, larger in area than the frontal area of the sphere, showed a minimum in the perturbed magnetic flux density just in front of the sphere. Behind the sphere the magnetic field was larger than the applied value decreasing to this value at larger axial distances from the body. Tamada's (1961) theoretical results show a similar distortion of the applied magnetic field.

(D) A body moving through a rotating or a stratified fluid creates regions of almost stangant fluid in front and behind in the neighbourhood of the axis. At larger radii there is a layer of fluid which has a velocity larger than the free-stream velocity; this layer decreases in thickness and increases in internal velocity as the body is approached. The flow sweeps over the equator and, depending on circumstances, can separate a little beyond the equator. Maxworthy (1968) shows this in some detail in one particular case. Such evidence is only suggestive and not essential to the development of a model.

Figure 6 displays a model which fits all of the known features of flows with

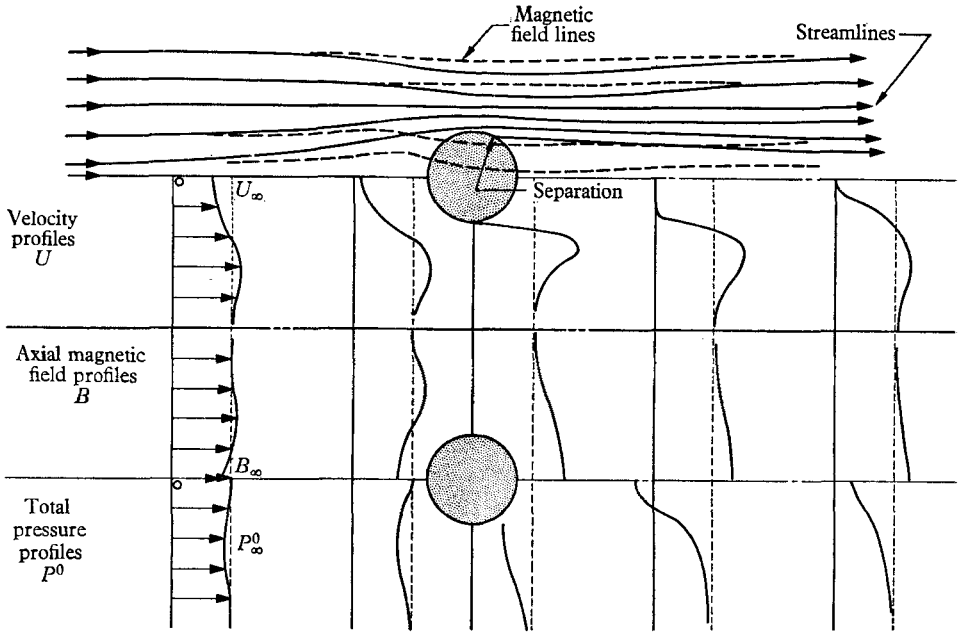

FIGURE 6. Model of the flow at large N showing approximate form of streamlines and magnetic field lines, qualitative radial distributions of velocity, axial magnetic field and total pressure at strategically located axial stations.

large N. The streamline and magnetic field line shapes have been exaggerated in order to make the character of the interactions clear.†

Starting from the observation of accelerated flows in the corresponding rotating fluid flow, it is known that there are no Coriolis forces available to accelerate the fluid directly and that such acceleration can only come from axial pressure gradients within the flow. It is now assumed that the axial pressure gradient is the driving mechanism in the present case.

For the almost parallel, inviscid flow away from the immediate neighbourhood of the body, the radial equation of motion reduces very simply to

$$\frac{\partial p}{\partial r} = j_\theta B_x \ddagger \quad \text{or on substituting for } j_\theta \quad \frac{\partial}{\partial r}\left(P + \frac{B_x^2}{2\mu}\right) = 0. \tag{1}$$

Wherever the flow concentrates the local magnetic field above the applied value, the static pressure falls below its value at infinity and vice versa, a fact which can be used in constructing static pressure profiles from the magnetic field profiles shown in figure 6. Care must be exercised in choosing a second equation, since not only must an acceleration of the flow take place, but a particle must also have lost total pressure by the time it reaches the body.

Following Tamada (1961) and Childress (1963), it is convenient to consider the behaviour of the total pressure along a streamline, and use the fact that P_∞^0 always decreases by an amount equal to the integrated Joule dissipation to the point in question. Once separation has taken place, viscous forces must be invoked to give the large loss in P^0 within the base region, and also allow the recovery of uniform conditions far downstream, as in ordinary flow.

These experiments have shown that a change in local static pressure reflects both a change in total pressure (due to Joule dissipation) and a change in velocity. Thus the accelerated flow shown in figure 6 and resultant deformation of the flow and magnetic field streamlines are consistent with the dynamics expressed in (1), in the change in P_∞^0, and the requirements of Ohm's Law that $j_\theta = \sigma U_r B_x$ and the Maxwell equation $\partial B_x/\partial r \approx \mu j_\theta$. Qualitative velocity, pressure and magnetic field profiles are also plotted in figure 6. Order of magnitude arguments given by Yonas (1966) indicate that these results are consistent with a layer type of solution which has a thickness of order $N^{-\frac{1}{4}}$ at a fixed axial location.

This inviscid outer flow, which has been constructed on the assumption that a rearward separated flow does exist, must now be matched to a magnetic boundary-layer flow which separates at the known separation point under the action of the outer flow pressure gradient. Near the nose, the boundary layer must have the character of a Hartmann type of layer modified as it moves around the equator in some as yet unknown way.

† Subsidiary experiments reported in Yonas (1968) have made it apparent that slug-like flows with virtually *straight streamlines* do exist at large N, and it is to this limiting case that this initial discussion is addressed. The results for $0 < N < 10$ will be discussed separately in later paragraphs.

‡ The subscripts x, r and θ refer to components of vectors in the axial, radial and azimuthal directions of a cylindrical co-ordinate system. Of course, the θ considered here is not the same as the θ used in the presentation of the pressure measurements. The latter, in a spherical co-ordinate system, would be the co-latitude of a point on the sphere surface

Also, note that the form of outer flow chosen is consistent with the known existence of the laminar separation point behind the equator. Efforts to put the present model on a less descriptive and more mathematical basis have not proved successful. That the work of Tamada (1961) does in fact predict some of the features of the inviscid flow that we have described is an encouraging sign. However, it must now be anticipated that the existence of a separated wake will have a far more drastic effect on the outer flow than even in the non-magnetic case. The fluid can signal far upstream that the conditions at the body are changed and that it now looks more like a sphere with a cylindrical afterbody than a whole sphere. The boundary conditions for Tamada's problem must be changed accordingly.

These experimental results bear the same relationship to the theoretical inviscid flow as results in ordinary flow do to the attempts to construct the ultimate laminar flow as R tends to infinity. In this case the situation may be slightly better since the oscillating drag measurements of Yonas (1968) indicate that wake disturbances must have very long wavelengths (at least 200 body diameters) as N becomes large. Some kind of quasi-laminar model may be appropriate.

Viscous effects must ultimately be important far downstream. It is anticipated that through the action of viscous stresses the velocity, total and static pressure will eventually become uniform and the wake will spread as an ordinary viscous wake, as shown by the Oseen solution for this region.

The transitional region, $1 < N < 10$, contains interesting features which can be explained using, basically, the simple physical ideas presented so far. The magnetic field tends to straighten streamlines; as the flow crosses field lines, Joule dissipation occurs and the fluid loses total head; there is a tendency to create a stagnant region surrounded by a layer of higher speed flow upstream of the body.

For low N the dissipative and retarding effects dominate, and the flow-straightening and accelerating effects are small. This is indicated by the decrease in velocity up to separation, a rapid increase in total pressure loss, and an increase in the base pressure. The only reason the overall drag increases is because a small stagnant region is beginning to be formed upstream and this causes an increase in the contribution from the front half of the sphere. Near the stagnation point the local velocities are very small and one would expect that a small magnetic field would have a disproportionate effect in this region where the *local* N is very large. However, as N continues to increase, acceleration and dissipation make both the minimum pressure and the base pressure more and more negative.

Mr Duncan Griffith maintained the sodium tunnel, designed and constructed the instrumentation; without his aid the present results would have been infinitely harder to obtain. His contribution was of inestimable value. Useful discussions with Dr G. Yonas are gratefully acknowledged.

This work represents the results of one phase of research carried out at the Jet Propulsion Laboratory, California Institute of Technology, under Contract no. NAS7-100, sponsored by the National Aeronautics and Space Administration.

REFERENCES

AHLSTROM, H. G. 1963 Experiments on the upstream wake in magneto-fluid dynamics. *J. Fluid Mech.* **15**, 2.

CHILDRESS, W. S. 1963 On the flow of a conducting fluid of small viscosity. *J.P.L. Tech. Rept.* 32–351.

FAGE, A. 1937 *A.R.C. R. & M.* no. 1766.

HORLOCK, J. H. 1963 Some two-dimensional magneto-fluid dynamic flows at low magnetic Reynolds number. *J. Fluid Mech.* **16**, 17.

LARY, E. C. 1962 A theory of thin aerofoils and slender bodies in fluids of finite electrical conductivity with aligned fields. *J. Fluid Mech.* **12**, 209.

MAXWORTHY, T. 1961 Liquid sodium flow facility for magneto-fluid dynamic research. *Rev. Sci. Inst.* **32**, 11.

MAXWORTHY, T. 1967 Experimental studies in magneto-fluid dynamics: Pipe flow through a solenoid of finite length. *J.P.L. Tech. Rept.* 32–1198.

MAXWORTHY, T. 1968 On the observed motion of a sphere through a short, rotating cylinder of fluid. *J. Fluid Mech.* **31**, 643.

TAMADA, K. 1961 On the flow of inviscid conducting fluid past a circular cylinder with applied magnetic field. *Cornell Univ. A.F.O.S.R. Rept.* no. 1087.

TAMADA, K. 1962 Flow of a slightly conducting fluid past a circular cylinder with strong, aligned magnetic field. *Phys. Fluids*, **5**, 7.

YONAS, G. 1966 Aligned fields, magneto-fluid dynamic flow past bodies. Ph.D. thesis, Calif. Inst. of Tech.

YONAS, G. 1968 Measurements of drag in a conducting fluid with an aligned field and large interaction parameter. *J. Fluid Mech.* **30**, 813.